

# Doing more with less: Realistic stereoscopic three-dimensional anatomical modeling from smartphone photogrammetry

Alex Morichon<sup>1</sup>  | Guillaume Dannhoff<sup>1,2</sup>  | Laurent Barantin<sup>1</sup>  |  
Christophe Destrieux<sup>1,3</sup>  | Igor Lima Maldonado<sup>1</sup> 

<sup>1</sup>UMR 1253, iBrain, Université de Tours, Inserm, Tours, France

<sup>2</sup>Centre Hospitalier Régional Universitaire de Strasbourg, Strasbourg, France

<sup>3</sup>CHRU de Tours, Tours, France

## Correspondence

Igor Lima Maldonado, UMR 1253, iBrain, Université de Tours, Inserm, 10 Boulevard Tonnellé, Tours 37032, France.  
Email: [limamaldonado@univ-tours.fr](mailto:limamaldonado@univ-tours.fr)

## Abstract

Traditional teaching methods struggle to convey three-dimensional concepts effectively. While 3D virtual models and virtual reality platforms offer a promising approach to teaching anatomy, their cost and specialized equipment pose limitations, especially in disadvantaged areas. A simpler alternative is to use virtual 3D models displayed on regular screens, but they lack immersion, realism, and stereoscopic vision. To address these challenges, we developed an affordable method utilizing smartphone-based 360° photogrammetry, virtual camera recording, and stereoscopic display (anaglyph or side-by-side technique). In this study, we assessed the feasibility of this method by subjecting it to various specimen types: osteological, soft organ, neuroanatomical, regional dissection, and a dedicated 3D-printed testing phantom. The results demonstrate that the 3D models obtained feature a complete mesh with a high level of detail and a realistic texture. Mesh and texture resolutions were estimated to be approximately 1 and 0.2 mm, respectively. Additionally, stereoscopic animations were both feasible and effective in enhancing depth perception. The simplicity and affordability of this method position it as a technique of choice for creating easily photorealistic anatomical models combined with stereoscopic depth visualization.

## KEYWORDS

anatomical models, anatomy, medical education, photogrammetry, stereoscopic vision

## INTRODUCTION

Complex tridimensional anatomy (3D) challenges both students and educators, as traditional teaching methods relying on stand-alone bi-dimensional representations often prove insufficient for a comprehensive understanding.<sup>1</sup> In this context, iterative laboratory dissection helps produce a realistic mental picture<sup>2-4</sup> but may be challenging to organize for large groups due to the requirements of sufficient specimens, dedicated facilities, and human resources. Additionally, due to legal, sanitary, or religious restrictions, the accessibility of anatomical specimens varies worldwide.<sup>2,5,6,7</sup>

Virtual 3D models and virtual reality platforms offer promising pathways to address this issue.<sup>8</sup> However, despite their increasing popularity in medical education over the past decade, these techniques come with their own challenges. One significant concern is that producing tridimensional models and setting up virtual reality stations also require dedicated equipment and significant investment,<sup>9</sup> making them inaccessible in underprivileged areas. Furthermore, viewing virtual 3D models on regular screens lacks immersion, realism, and stereoscopic vision, underscoring the need for more realistic, widely accessible alternatives.

In an effort to enhance accessibility through simplicity and affordability while ensuring a high degree of fidelity, we have recently

been able to produce and display lifelike 3D models by combining inexpensive procedures: smartphone-based 360° photogrammetry, virtual camera recording, and stereoscopic display. The final models displayed remarkable realism, clearly surpassing artificial computer-generated models. In the present study, we assessed the feasibility of this method through a comprehensive examination, challenging it with different specimen types: osteological, soft organ, neuroanatomical, regional dissection, and a dedicated 3D-printed phantom. The results were discussed in the light of existing literature, recent developments in photogrammetry, and its applications in anatomical education.

## METHODS

### Selection of anatomical specimens

Anatomical specimens were collected from our institution's body donation program. Each donor received detailed information and provided written proof of their consent for using their bodies or parts of them for educational and research purposes. The present study followed the latest local and international regulations regarding research using human specimens.

Different anatomical parts were selected to enable an extensive assessment of the possibilities of photogrammetric reconstruction of anatomical models. The following elements with very distinct shapes, consistencies, textures, and colors were included:

1. *Bone*. A dried right human hip bone was used. It was prepared by successive boiling cycles, meticulous cleaning, and bleaching with hydrogen peroxide.

2. *A soft organ*. A non-dissected heart was extracted after the whole body was fixed through intracarotid injection of 2.6 L of formal-based commercial preservation solution (Arthyl-25, Hygecobel, Garges-lès-Gonesse, France) and preserved in formaldehyde solution pending its use. Besides causing fixation, formalin increases tissue rigidity, facilitating positioning, and photogrammetric 360° image acquisition.
3. *A cerebral hemisphere*. A left specimen was used. The brain was fixed through slow bilateral carotid injection of 1.5 L of 10% formalin and preserved in a formaldehyde solution pending its use.
4. *A dissection specimen*. Dissection of the right hand, wrist, and forearm in fresh condition was performed. The different planes were dissected from the surface to the depth according to the anatomical limits classically quoted<sup>(10)</sup>. The skin covering, subcutaneous adipose tissue, and antebrachial fascia were resected to expose the underlying muscular and vascular-nerve structures of interest.

### Photogrammetry and three-dimensional modeling

The anatomical specimens were photographed with an OPPO Reno-4 Z 5G smartphone (BBK Electronics, Canton, China). Each specimen was placed on a small table covered with a black background. This configuration allowed the operator to navigate freely around the specimen and place it in a location with proper vertical illumination. A fixed reference centimetric quadrangular piece of gray-painted cardboard was placed in the field of view to facilitate image alignment during photogrammetry (Figure 1).

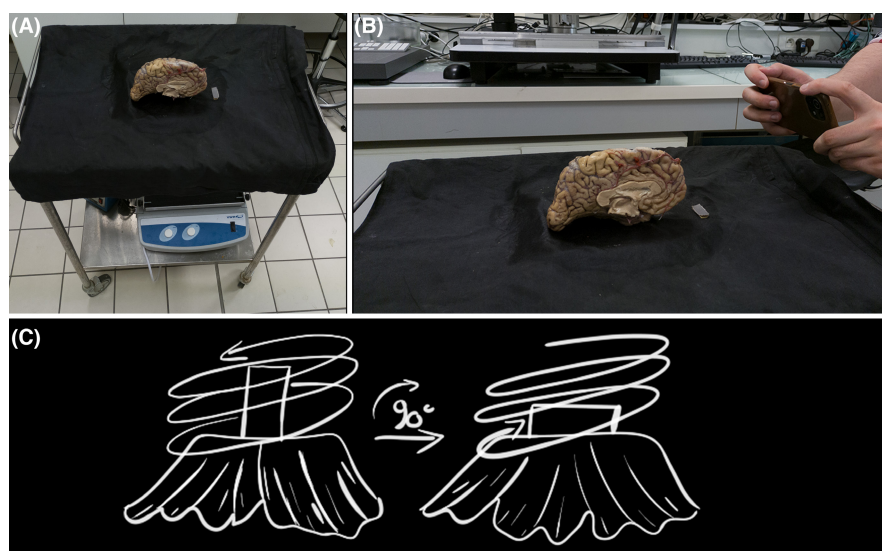


**FIGURE 1** Setting for photographic acquisition using a smartphone. (A) The object to be scanned is placed on a small table allowing the operator to move around. A black background is used, and a fixed reference centimetric quadrangular piece of gray-painted cardboard is placed in the field of view to serve as a reference for photogrammetry. (B) The photography procedure is then carried out freehand. (C) The camera's path is an ascending spiral where the shots are taken at roughly regular intervals. The position of the specimen is then changed to enable all its aspects to be photographed and the acquisition re-starts in a descending spiral. The total number of photographs per specimen varied between 70 and 200.

The smartphone camera settings were configured as follows: F2 aperture, ISO 200 sensitivity, EV 0.0 exposure value, and no flash. The exposure time was not adjustable. The acquisition process was conducted without camera support, with the operator holding the phone and moving around the anatomical specimen. A consistent distance of approximately 30 cm between the smartphone lens and the specimen was maintained.

The camera movements followed an ascending spiral pattern, capturing shots at relatively uniform intervals. This spiral motion commenced at an angle close to  $-30^\circ$ , measured between a plane parallel and a straight line connecting the photographic lens to the object. Subsequently, the operator continued to move the camera at intervals as consistently as possible, completing three spiral cycles and ending at an angle of  $+30^\circ$ .

Following this initial phase, the specimen was rotated by  $90^\circ$  along one of its axes to ensure comprehensive coverage of all aspects. The acquisition process then recommenced, following the same procedures but in a descending spiral motion. The total number of photographs taken per specimen ranged from 70 to 200 or 35 to 100 per spiral movement.

For photogrammetry, we used the KIRI Engine software (KIRI Innovations, Toronto, Canada), a free application for iOS and Android mobile operating systems (inexpensive paid features are also available and were used for the forearm and test-object reconstructions) that uses a dedicated server for reconstruction. The application uses artificial intelligence algorithms to reconstruct an object in 3D based on the photographs. Generally, the more pictures taken around the object at different angles, the better the application deduces the object's shape. Given the large amount of data involved, the processing occurs via the application's servers, allowing for faster modeling. The following reconstruction settings were used: (i) raw data storage (allowing access to the original photographs in case of a poor reconstruction); (ii) number of faces in the mesh: high; (iii) texture quality: high; (iv) output file format: .fbx; and (v) object detection via artificial intelligence (allowing the application to detect changes in object position). The 3D mesh and textured model were then generated, and the .fbx model was exported onto a laptop (settings: retopology, quad number target 100%, curve ratio target 90%).

## Phantom testing

To objectively challenge the method, a phantom with different complex elements was designed and 3D-printed. This phantom was designed using Fusion 360 software (Autodesk, San Rafael, USA), sliced for printing using Cura software (UltiMaker, Utrecht, Netherlands), and printed in several assemblable parts using an UltiMaker2 3D printer (UltiMaker, Utrecht, Netherlands) in gray polylactic acid and white acrylonitrile butadiene styrene. It was then assembled using conventional instant cyanoacrylate glue (GreenStuffWorld, Alicante, Spain) and completed with additional materials (wood, leather, and carpet) corresponding to specific challenges for photogrammetric reconstruction.

The criteria for selecting the testing phantom's morphology were thoughtfully curated to rigorously evaluate photogrammetric reconstruction. These criteria included complexity, printability, rigidity for acquisition comparability, and a hollow shape mimicking challenges found in human anatomy, as detailed below. In response to acquisition difficulties in areas with reduced light penetration due to cavities and angles, we opted for a hollow cubic form enriched with diverse morphological features. With two fewer walls, this shape allows us to assess the method's ability to capture internal angles without introducing rounding artifacts. Additionally, we introduced a smooth, white, and reflective face to evaluate the method's performance on such reflective surfaces.

The phantom took the form of a 60 mm cube with two adjacent faces missing. The external configuration of the four faces was the following: (i) a series of 2-mm-thick crossbars of decreasing intervals of 2, 1, 0.5, 0.33, 0.1, 0.2, and 0.05 mm (for resolution testing); (ii) a white reflective surface polished with acetone vapors (Merck, Darmstadt, Germany) and coated with clear varnish (for testing with bright, smooth surfaces, which are non-rarely encountered in anatomical specimens); (iii) three strips of wood, leather, and gray carpet (representing the roughness of bone, the texture of human skin, and irregular hairy areas, respectively); and (iv) an irregular surface adorned with high reliefs of different sizes and 10, 8, 6 and 4 mm hemispheres (to challenge the reconstruction process with structures of complex shapes of different sizes as are usually encountered during dissection). Two parallel faces of the cubic phantom were pierced with four holes, allowing the installation of a natural hemp rope (diameter 3 mm) suspended between two faces at different heights and depths. This last feature aimed to test reconstruction capabilities for suspended elements and the recognition of small fibers. A support bar was added to prevent the collapse of the global structure.

Five  $360^\circ$  image acquisitions of the testing phantom were conducted to assess the accuracy of reconstructions in terms of mesh resolution, texture, and reproducibility. The mesh resolution was assessed in the decreasing spaces between the crossbars on one side of the object. Texture accuracy was assessed similarly. We sought the smallest of these spaces with a color difference clearly visible to the naked eye. Iterative measurements of mesh reproducibility were taken on the hemispheres to quantify the variability among the five acquisitions. Measurements, number of mesh faces, and texture characteristics were obtained using Meshlab (CNR-ISTI, Pisa, Italia). The mean number of faces of the obtained meshes was calculated for different mesh qualities: low-poly, classic, and retopo+.

## Stereoscopic display

To combine stereoscopic vision and 3D modeling, each .fbx file was displayed using the anaglyph method in the free Agisoft Viewer (Agisoft LLC, St. Petersburg, Russia). This procedure allowed the user to move the object freely while enjoying a 3D display.

To enable stereoscopic visualization without an external viewer, stereoscopic rotating high-definition videos were generated (both anaglyph and side-by-side). Blender software (Blender Foundation, Amsterdam, Netherlands), a free 3D modeling application, was used for this purpose. A horizontal virtual camera angle and three-source lighting (left, right, and anterior) were defined. The animation was programmed to sequentially display models from anterior, left, posterior, right, superior, and inferior views. The virtual camera was set to parallel stereoscopy mode with a parallax equivalent to 1/30 of the model-camera distance.

## RESULTS

### Meshing and morphology reproduction

By employing a smartphone and photogrammetric reconstruction, the freehand photograph procedure efficiently merged the image series and removed the background. All the aspects of all specimens could be acquired. In the specific case of the dissected forearm, a very soft and mobile specimen, a total of three 3D models were reconstructed: (i) the whole specimen in the supine position with flexion-adduction of the second to fourth fingers on the palm of the hand; (ii) its anterior aspect in a supine position with extension-abduction of all the fingers (in conformity with the anatomical position); (iii) its posterior aspect in a supine position with semi-flexion of the second to fourth fingers on the palm of the hand. The set of 3D models enabled assessment of the method's ability to reconstruct surfaces of different natures, such as smooth, highly reflective, irregular, and complex. Examining anatomical details of various shapes, sizes, and relative positions allowed for the assessment of the method's ability to differentiate them and provide a sense of depth. Table 1 summarizes the key attributes of the 3D models alongside their corresponding stereoscopic videos.

Areas that were impossible to scan (e.g., the depth of a narrow brain sulcus) were rare, and the impact on the final result was minimal (see below). No significant macroscopic reconstruction errors or artifacts hindering the quality of the resulting mesh were identified. The method was accurate in reproducing the main morphological features of the specimens, which are described in more detail. The resulting 3D models and photographs are shown in Figures 2–6 to allow visual comparison. To enable the models to be opened without specific viewing software, they are presented in PowerPoint files that are available in the Supplementary Materials (download required for proper viewing). The .fbx source files are also available for download.

The hip bone is a paired symmetrical structure that contributes to the formation of the bony pelvic girdle and the bony pelvis along with the sacrum. The bleached bone presents a rough, granular texture. Exhibiting a complex 3D conformation, it features numerous variably accentuated reliefs. In the photographs, smaller anatomical features, muscle attachment points, and millimetric vascular

**TABLE 1** Key attributes of seven 3D models and corresponding stereoscopic videos produced from smartphone photogrammetry of different types of anatomical specimens and a testing object.

3D models <sup>a</sup>		Stereoscopic videos <sup>b</sup>					
Faces	Vertices	Texture	Size (Mb)	Resolution	fps	Anaglyph file size (Mb)	Side-by-side file size (Mb)
Right coxal bone	88,436	4096 × 4096	19.21	1920 × 1080	24	2.23	3.78
Heart	118,220	4096 × 4096	24.98	1920 × 1080	24	3.31	6.58
Left hemisphere	148,796	4096 × 4096	29.10	1920 × 1080	24	2.63	4.43
Right forearm—anterior	188,172	4096 × 4096	31.93	1920 × 1080	24	2.19	3.57
Right forearm—posterior	176,062	4096 × 4096	30.54	1920 × 1080	24	2.04	3.31
Right forearm—full	346,979	4096 × 4096	29.1	1920 × 1080	24	1.90	3.20
Phantom—no rope	136,335	4096 × 4096	37.53	1920 × 1080	24	3.31	5.43
Phantom—rope	589,521	4096 × 4096	43.78	1920 × 1080	24	6.31	10.52

Abbreviation: fps, frames per second.

<sup>a</sup>Retopology<sup>†</sup> modeling, .fbx files.

<sup>b</sup>22 s, .avi files.

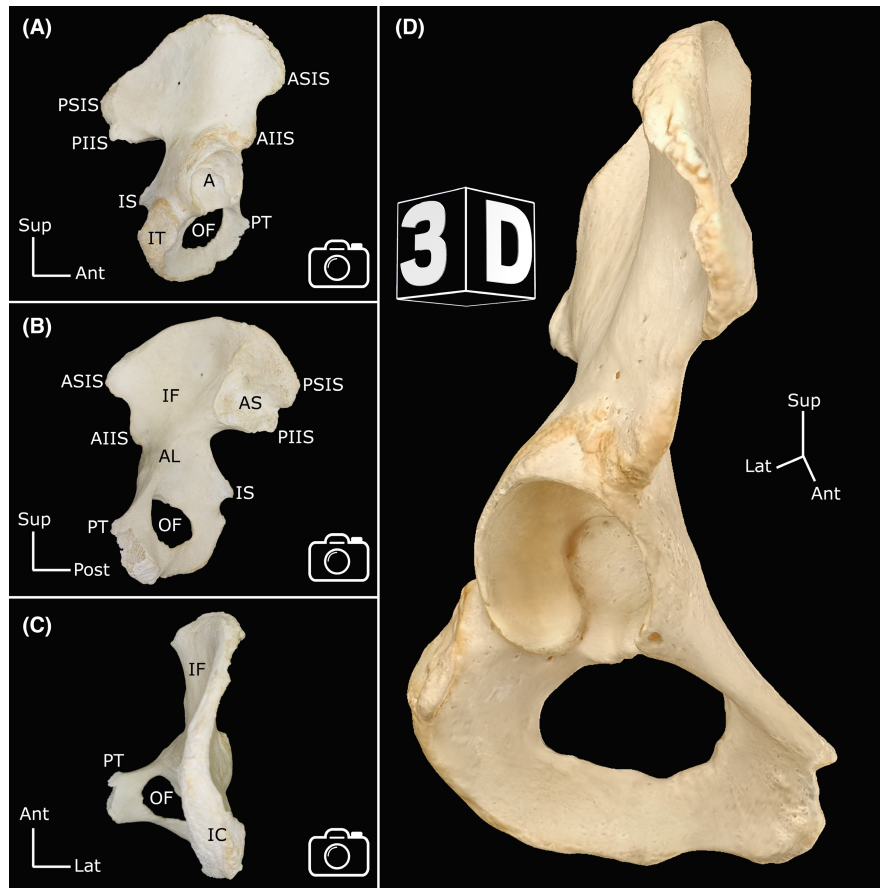


**FIGURE 2** 3D model of a human bone: a bleached right hip bone. (A–C) Photographs from different perspectives: lateral (A), medial (B), and superior (C) views. (D) Screenshot showing the corresponding 3D model obtained from smartphone-based photogrammetry. A, acetabulum; AL, arcuate line; AIIS, anterior inferior iliac spine; AS, auricular surface; ASIS, anterior superior iliac spine; IC, iliac crest; IF, iliac fossa; IS, ischial spine; IT, ischial tuberosity; OF, obturator foramen; PIIS, posterior inferior iliac spine; PSIS, posterior superior iliac spine; PT, pubic tubercle.

foramina were clearly visible and accurately replicated without difficulty (Figure 2 and Supplemental 3D Model 1).

The heart is a single intra-thoracic organ, the keystone of blood circulation. It has a relatively smooth, very shiny, and reflective surface due to the presence of the epicardium. The color varies from purple-gray to light yellow, depending on the amount of adipose tissue on the cardiac surface. Again, smaller anatomical details were reproduced appropriately, including the tiny pericardial folds of the ventricular and atrial surfaces (Figure 3 and Supplemental 3D Model 2). Part of the lumen of the great vessels and cardiac cavities was captured and visible.

The cerebral hemisphere comprises the telencephalon and diencephalon. In the specific case of the specimen used in this study, the brain stem was sectioned so that the upper part of the mid-brain was also preserved. The hemisphere has a highly contoured, finely granular, and shiny surface with a brownish color. The sulco-gyral anatomy was accurately revealed, such that all macroscopic sulci could be readily identified in the 3D model. Structures of the medial aspect of the cerebral hemisphere, such as the fornix, corpus callosum, and thalamus, were also accurately reconstructed (Figure 4 and Supplemental 3D Model 3). The application was able

to reconstruct deep depressions when they were large enough for the camera to capture their floors. In some specific sulci, narrow, deep depressions were impossible to reconstruct (e.g., depth parts of the central or lateral sulcus). The application obturated them with a mesh plane, covered by a texture, at varying depths, depending on the available data. It is important to note that those areas were only visible with manipulation, even in the anatomical specimen.

The right-sided forearm was sectioned in its proximal portion for the purpose of the present study. Thus, the dissection involved most of the forearm, the entire wrist, and the hand. The dissection was relatively superficial to reveal musculotendinous and vascular-nervous elements (e.g., brachioradialis and digital extensor muscles, radial and ulnar arteries, median, and ulnar nerves) and enable assessment of the method's topographical reconstruction capabilities. All those structures of various shapes and textures were adequately reconstructed (Figure 5 and Supplemental 3D Model 4).

Regarding the phantom, the number of faces was as follows:  $14,907 \pm 207$  (mean  $\pm$  SD) for the low-poly,  $183,360 \pm 27,511$  for the classic, and  $251,803 \pm 32,858$  for the retopo<sup>+</sup> meshing model. Using the same 3D object generation protocol applied to anatomical

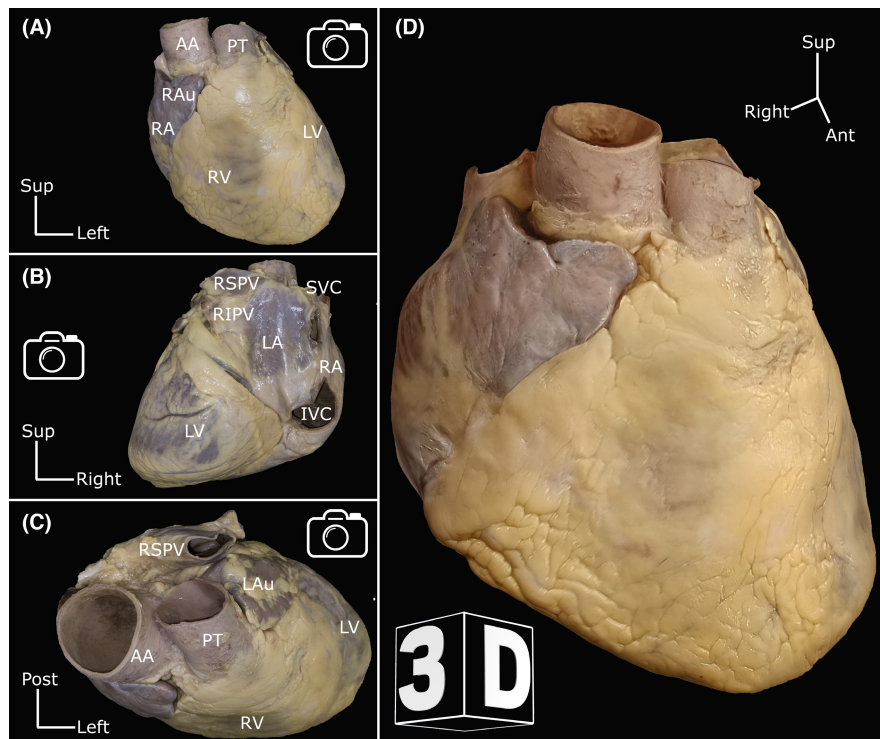


**FIGURE 3** 3D model of a human intra-thoracic organ with a smooth and reflective surface: the heart. (A–C) Photographs from different perspectives: anterior (A), posterior (B), and superior (C) aspects. (D) Screenshot showing the corresponding 3D model obtained from smartphone photogrammetry. AA, ascending aorta; IVC, inferior vena cava; LA, left atrium; LAu, auricle of the left atrium; LV, left ventricle; PT, pulmonary trunk; RA, right atrium; RAu, auricle of the right atrium; RIPV, right inferior pulmonary vein; RSPV, right superior pulmonary vein; RV, right ventricle; SVC, superior vena cava.

specimens, the mesh reconstruction resolution was around 1 mm (median 1, range 1–2). Mesh reproducibility was assessed using the measured diameters of the hemispheres and their variation among acquisitions. The maximum overestimation observed was 0.76 mm (in a 10 mm sphere). Overestimations in diameter were observed regardless of the sphere's size, while underestimations were only observed with the smallest 4 mm sphere. These results are detailed in Table 2. The suspended elements in confined spaces (ropes inside the cube) were identified as the main constraint for acquisition and reconstruction (Figure 6 and Supplemental 3D Model 5). The reconstruction also struggled with long, straight, and parallel lines.

## Texture

All the reconstructed models exhibited photorealistic textures to the naked eye. For the most demanding acquisitions, we were able to successfully reproduce the following surfaces: smooth and shiny (e.g., epicardium, cartilage), including wet, rough, matte, and hilly (e.g., bone tubercles, hemispheric cortex); reflective and cracked or slightly irregular (e.g., skin, adipose tissue); complex and fibrous (e.g., tendons, fascias); and artificial hairy surfaces. The textures' appearances were very similar to the reference photographs.

However, some texture elements were imperfect. Due to the uneven lighting (inherent to a freehand image acquisition procedure), the

reconstruction merged different exposure tones to create a texture. Darker areas thus appeared on parts of the specimen in contact with the support. These corresponded to the junctions between the two series of images obtained before and after the 90° tilt of the specimen, which was necessary for its complete reconstruction. The result was a darker texture at these junctions than in the rest of the model.

A close examination was made by the naked eye of the colorimetric differences in the decreasing spaces between the crossbars on one of the model's faces to assess the texture resolution. The median texture resolution over the five acquisitions was 0.10 mm (median, range 0.10–0.20). The texture of each model was produced in 4096 × 4096 pixels.

## Stereoscopic display

All 3D anatomical models could be successfully displayed in both red-cyan anaglyph and side-by-side stereoscopic modes. Both stereoscopic modes successfully offered depth perception while allowing for an accurate and immersive representation of 3D objects and the ability to rotate them. Due to the very nature of stereoscopic methods, slight color modification was observed during display in anaglyph mode (Figure 7).

To produce files that could be viewed without specific 3D model readers, stereoscopic recordings of the 3D models

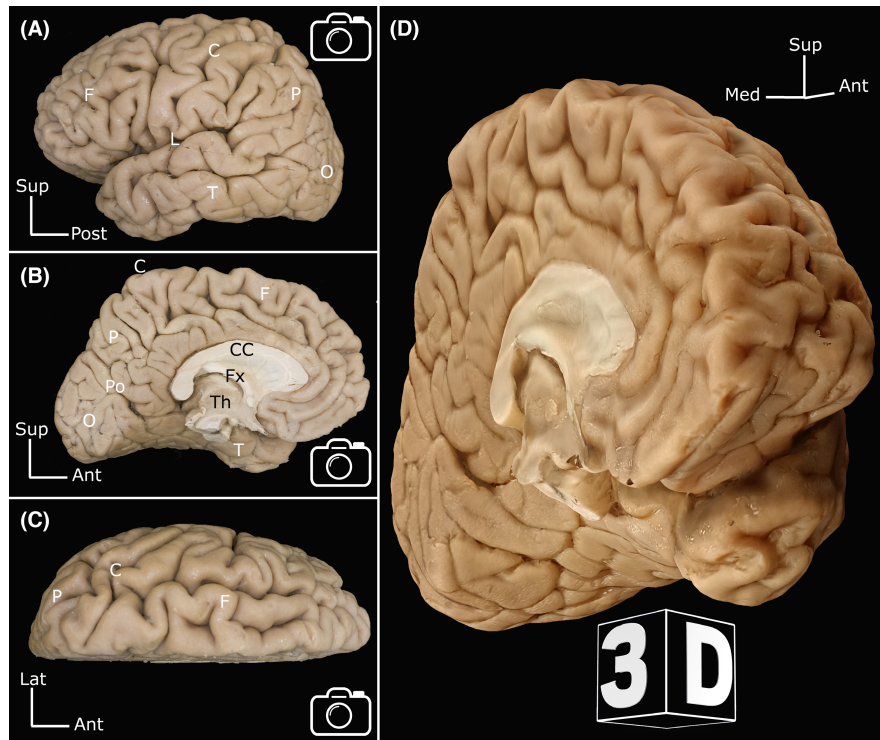


**FIGURE 4** 3D model of a human intracranial structure with an irregular surface: a left cerebral hemisphere. (A–C) Photographs from different perspectives: anterior (A), posterior (B), and superior (C). (D) Screenshot of the corresponding 3D model obtained from smartphone photogrammetry. C, central sulcus; CC, corpus callosum; F, frontal lobe; Fx, fornix; L, lateral fissure; O, occipital lobe; P, parietal lobe; T, temporal lobe; Th, thalamus.

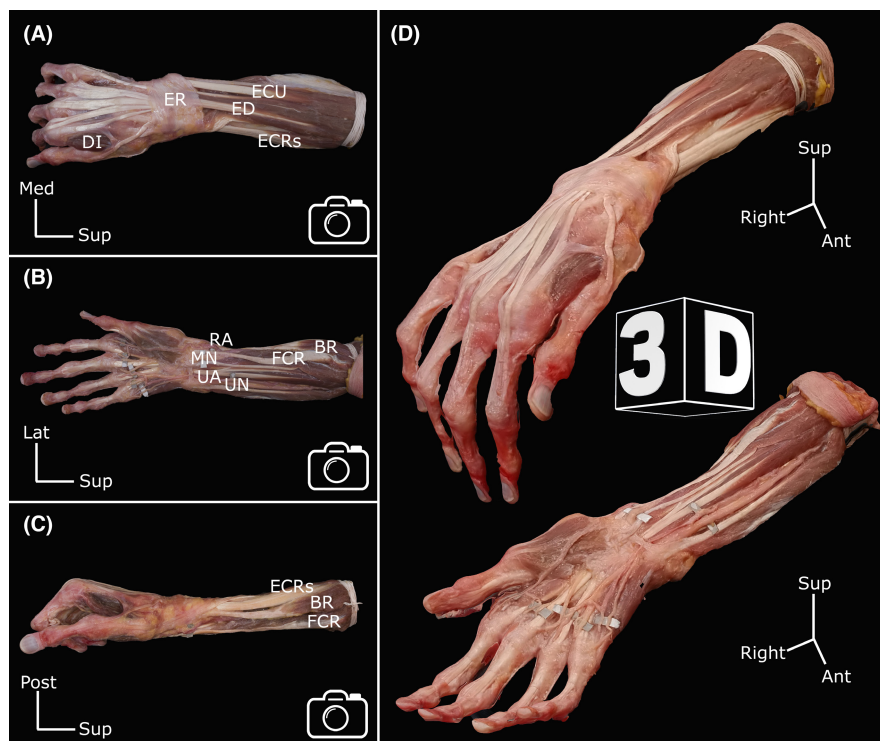


**FIGURE 5** 3D model of a dissected region: a right forearm, wrist, and hand. (A–C) Photographs from different perspectives: posterior (A), anterior (B), and lateral (C). (D) Screenshot of the corresponding 3D model obtained from smartphone photogrammetry. BR, brachioradialis; DI, dorsal interossei; ECRs, extensor carpi radialis brevis/longus; ECU, extensor carpi ulnaris; ED, extensor digitali; ER, extensor retinaculum; FCR, flexor carpi radialis; MN, median nerve; RA, radial artery; UA, ulnar artery; UN, ulnar nerve.

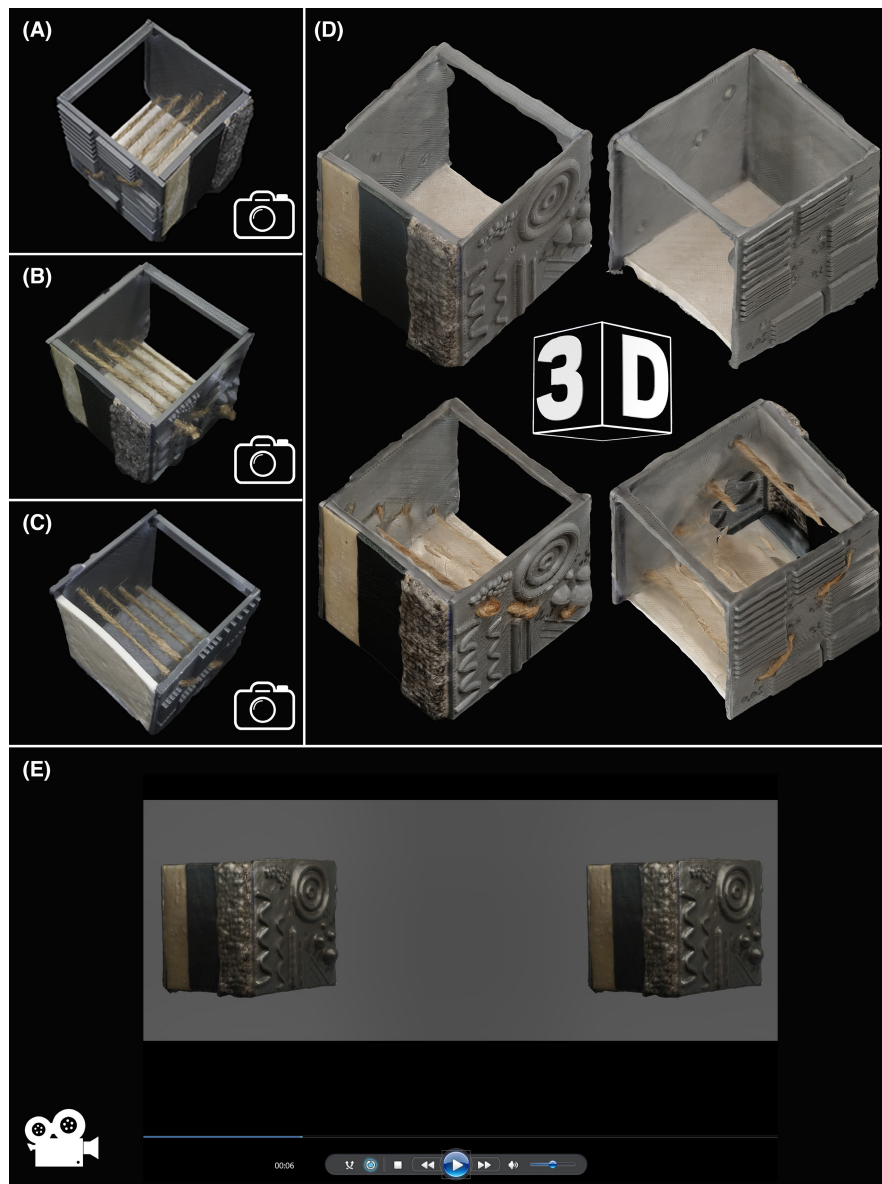


**FIGURE 6** 3D model of the 3D-printed phantom. (A–C) Photographs from different perspectives. (D) Screenshots of the corresponding 3D model with (bottom) and without (top) suspended ropes used for further testing. (E) Screenshot of the side-by-side (left–right) stereoscopic animation of the rotating 3D model.

**TABLE 2** Summary of measurements obtained from five 3D virtual models generated via smartphone-based photogrammetry of the same physical object: a testing phantom.

Acquisitions	Number of faces	Resolution		Measurements (mm)			
		Mesh	Texture	10mm sphere	8 mm sphere	6 mm sphere	4 mm sphere
1st	243,618	2	0.2	10.47	8.36	6.33	3.64
2nd	209,218	1	0.1	10.76	8.05	6.04	3.85
3rd	238,908	2	0.1	10.22	8.39	6.35	4.13
4th	272,568	1	0.1	10.24	8.23	6.26	4.14
5th	294,707	1	0.2	10.45	8.12	6.18	3.62
Median	–	1	0.1	–	–	–	–
Mean	251,804	–	–	10.43	8.23	6.23	3.88
SD	32,858	–	–	0.22	0.15	0.13	0.25

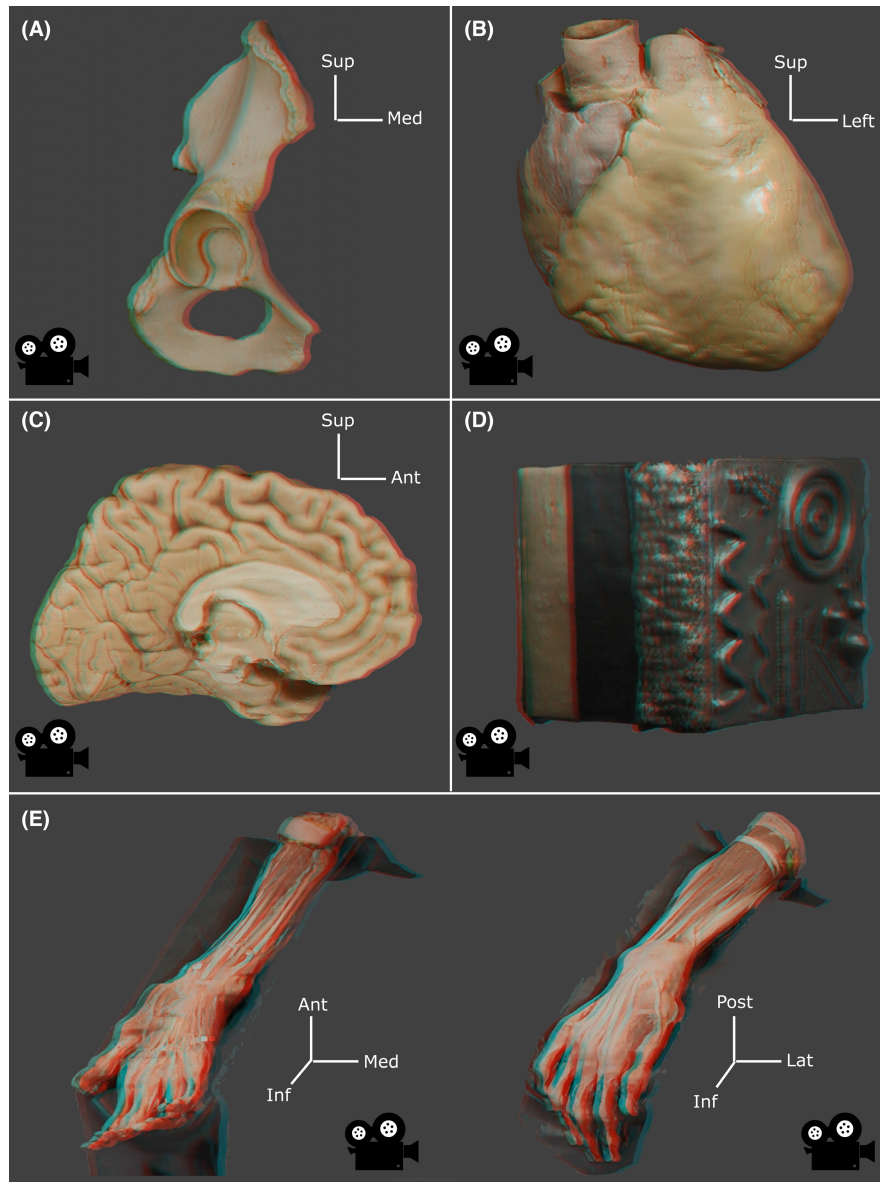


**FIGURE 7** Screenshots of anaglyph stereoscopic animations anatomical 3D models obtained from smartphone-based photogrammetry. These animations display all model faces by rotation. (A) Right coxal bone. (B) Heart. (C) Left cerebral hemisphere. (D) 3D-printed phantom. (E) Right forearm. Stereoscopic animations are available for download in the supplementary material in both anaglyph and side-by-side modes.

were easily obtained. Two stereoscopic videos were produced in red-cyan anaglyph (displayable on any regular screens) and side-by-side (displayable on virtually any color screens and also projectable) modes for each model. The image freezes for 2.2 s in each perspective, so a simple pause can enable a more detailed study of each model's aspect in the stereoscopic environment. Stereoscopic videos are available for download as part of the [Supplementary Material](#).

### Temporal and financial costs

The global procedure of 3D reconstruction was accessible due to its simplicity and low cost. The acquisition procedure for one specimen

took 5 to 6 min, and the export-reconstruction step took between 5 and 15 min. The creation of stereoscopic video animations was the most time-consuming procedure, taking between 2 and 4 h per animation. The total processing time for a specimen, from acquisition to the export of a final stereoscopic file varied from 2 h and 15 min to 4 h and 50 min.

Financial costs were minimal. A free application was used for modeling. The software used for the manipulations conducted on the computer was also free. For stereoscopic visualization, cardboard anaglyph glasses were obtained online for <1 USD each. As smartphones and computers (basic models are required) are relatively widespread today, the cost of these devices was not considered as part of the cost of the procedure. If unavailable, they should be added to the total cost required.

The KIRI Engine application offers a nonobligatory subscription (starting at approximately 50 USD per year) if the user wants to use a greater number of photographs for better-quality results. The use of the side-by-side option for stereoscopic projection or display on a 3DTV may also require investment in equipment, which varies considerably depending on the specific purposes and audience size.

## DISCUSSION

Teaching the anatomy of three-dimensional complex structures is frequently a challenging task. In such circumstances, it becomes crucial to recognize the continually changing landscape of educational resources. However, many of the modern tools still come with drawbacks. This is the case, for example, with augmented reality tools that often demand substantial investment, or artificial models that, more often than not, lack microanatomical details. We propose an alternative solution combining photogrammetry and stereoscopy to produce realistic 3D anatomical models simply and inexpensively. The resulting models have a high morphological and textural accuracy, and the exported files are easily shareable.

A common problem in reconstructing models from anatomical specimens is the presence of blind zones corresponding to points of contact between the specimen and its support. Our proposed method does not present this inconvenience since it can merge different acquisitions to obtain a complete 3D model. The specimen can be moved between acquisitions as long as it is not deformed. Besides the very realistic texture, the use of real specimens for image acquisition ensures an anatomically correct and rich 3D model.<sup>11,12</sup> This benefit is one of the main distinctions of this method as compared to the approximative or sometimes inaccurate computed-generated objects.<sup>13,14</sup>

An issue frequently observed in current anatomical 3D model applications is the tendency to separate structures by freeing them from peri-organic spaces, cellulosic tissue, fascias, and sheaths. This practice can be useful for studying basic anatomy but is often insufficient for in-depth studies such as those needed by specialists and surgeons. The delicate balance between structure individualization and the preservation of realistic anatomical relationships is critical in this situation. These parameters can be easily modulated in 3D models generated from the photogrammetry of dissected specimens. The shape and texture of models can be modified by any operator using 3D modeling software. This possibility opens an avenue for more advanced pedagogical uses, as it enables texture modifications or the detachment of structures if needed for didactic reasons.

There are currently several ways of obtaining 3D models from real anatomical data. Surface scanning is implemented mainly by laser scanners and structured light scanners. These use either reflection (by trigonometric triangulation) or deformation of the light emitted to recreate the studied object in 3D. These techniques are usually fast and accurate but can be hampered by the tonality of

ambient light, representing a significant logistical and financial constraint. Another option is 3D reconstructions based on CT or MRI datasets,<sup>8,15,16</sup> a method that provides the advantage of enabling the reconstruction of inner surfaces. The process is inexpensive if the operator has access to imaging data. However, segmentation may be very time-consuming, and the accuracy, particularly of small structures, may not be optimal. It is worth noting that the methods described above produce untextured models and demand complementary procedures to create an artificial texture.

Multiple photographs are required during photogrammetry to faithfully reconstruct textures. Photogrammetry was initially used for aerial cartography and has been used for over a decade within the archaeology/paleontology community.<sup>17-19</sup> It is a low-cost technique compared to methods using surface lasers. It is very accurate if the initial photographs are of sufficient quality, but it requires considerable digital resources to ensure 3D reconstruction from the images. This technology has the advantage of being available on smartphones using several free applications.

Another 3D reconstruction technology available on smartphones is LIDAR (light detection and ranging). Like photogrammetry, this solution is derived from aerial cartography/topography; it is based on the real-time emission and reception of pulsed electromagnetic waves. However, smartphone photogrammetry seems to have a better and relatively constant resolution, while LIDAR obtains less consistent results with variable precision depending on the size of the scanned objects.<sup>20</sup> For now, LIDAR technology is mainly used in Apple products, but it is destined to become more widespread in the future. Some applications use a combination of photogrammetry and LIDAR technologies to improve their reconstruction capacities.<sup>21</sup>

Studies in the literature proposing 3D modeling of organs and anatomical regions (including with photogrammetry) are sparse but increasing.<sup>8,22,23</sup> Most photogrammetry studies propose models of varying precision using techniques that require a dedicated platform and investment.<sup>9,24</sup> Some have already suggested the use of smartphones,<sup>21,24,25</sup> but, to our knowledge, no study to date has proposed a combination of smartphone photogrammetry of real specimens and stereoscopic techniques nor challenged the photogrammetry with a testing phantom. In addition to the quality of the models obtained, the strength of the technique presented here lies in its simplicity and low cost. With this relatively simple method, virtually any laboratory can create and share high-quality realistic stereoscopic anatomical 3D models and display them stereoscopically on commonly used digital platforms.

Our decision to utilize the Kiri Engine application was based on its ability to produce realistic reconstruction results and its comprehensive control over the reconstruction process. Although other alternative smartphone-based photogrammetric reconstruction applications exist, such as Qlone (EyeCue, Yokneam, Israel), Polycam (Polycam, San Francisco, USA), RealityScan (Epic Games, Cary, USA), and WIDAR (WOGO Inc., Tokyo, Japan), a comparative analysis among them falls outside the scope of this study. Nevertheless, it is crucial to recognize that the outcomes of photogrammetric reconstruction may vary depending on the selected application and the

quality of the smartphone camera. Consequently, we recommend that users explore different applications to optimize their selection based on the specific capabilities of their smartphone and the characteristics of the structures they intend to scan.

Different methods can be used to share 3D models. For instance, 3D models can be easily used to create interactive slides. A common use is to share these models, which may also be annotated on specialized online platforms.<sup>11,12</sup> Other options include iBooks, eBooks, or 3D .pdf files, depending on the local and final purpose (e.g., reading vs. lecturing).<sup>8</sup> The fast-advancing augmented reality or virtual reality technology has also started to provide interactive solutions for these media.<sup>14,26-28</sup> Some video game tools, such as Unity or Unreal Engine, can create interactive situations using 3D models, sometimes in conjunction with augmented or virtual reality.<sup>29,30</sup> The adoption of 3D-printed models derived from three-dimensional medical image datasets or surface scans is gaining significant momentum in both anatomy teaching.<sup>31-33</sup> and pre-operative planning,<sup>34,35</sup> offering an alternative approach for physical visualization.

The 3D models obtained by the technique described here are exported in .fbx format, which integrates a texture and can be easily shared with a large audience by standard means of file transmission. On smartphones and tablets, the augmented reality option allows the model to appear in the student's working environment if desired.<sup>21</sup> Another inexpensive option is to display anatomical models using the Google Cardboard VR platform (Google LLC, Mountain View, USA) for <1 USD. After the smartphone is placed into the cardboard device, the user can then freely turn the virtual object around with the help of a free VR application.

One important factor that enhances the immersive nature of the produced content is stereoscopic visualization. Sir James Mackenzie Davidson, an English physician, first demonstrated the clinical potential of stereoscopy in medicine (radiography) in 1898, 3 years after Wilhelm Conrad Röntgen's discoveries about the x-ray. He detailed a successful application of stereoscopy in locating a bullet lodged in the leg of a 14-year-old boy.<sup>36</sup> Since then, the adoption of stereoscopic viewing has progressively expanded throughout the medical field. This evolution included various technical variants in the last decades such as the View-Master device (initially designed as a toy), anaglyphs, and methods based on polarized light projection.<sup>37-41</sup>

Animations of 3D models using the red-cyan anaglyph technique enable stereoscopy with a modest investment: the purchase of 3D anaglyph glasses available for <1 USD for the cheapest models. Instructors can then distribute models and animations even to large groups of students. Indeed, such 3D models fit perfectly into current digital teaching methods via e-learning platforms or massive open online courses (MOOC). The projection of (side-by-side) stereoscopic videos enable very realistic perception rendering either with passive (polarized light) or active (higher cost) 3D glasses. Static stereoscopic images can also be easily produced from captures of different (left and right) perspectives of a virtual object.<sup>38</sup>

Radiological techniques, such as CT and MRI, can provide 3D views through volume rendering, surface rendering, or a combination of both. Many authors have underscored the utility of these

methods in the context of anatomy education.<sup>42-51</sup> It is essential to emphasize the distinctions between the approach we propose and these methods and the fact that they serve different objectives and are complementary. One crucial distinction concerns texture. Photogrammetric reconstructions offer the student an appearance closely resembling photographs of the actual specimens. Factors like color, brightness, and apparent moisture are readily discernible. These specificities are not evident in objects generated from radiological images. While applying textures to these objects is feasible, they currently fall short of replicating the realism and diversity of human tissue appearances.

Cinematic rendering represents a pioneering advancement in medical imaging, conferring unique advantages over conventional volume rendering methods.<sup>52-54</sup> It employs complex lighting and shading algorithms inspired by the film industry to create visually captivating and detailed images. By simulating light interaction with tissues and structures, cinematic rendering intensifies the perception of realism. This technique offers an intuitive, lifelike representation of anatomical structures. Nevertheless, cinematic rendering does have limitations. A significant constraint lies in its computational complexity, demanding substantial processing power and time. Generating high-quality cinematic renderings can be time-intensive and resource-demanding, hindering real-time applications. Furthermore, cinematic rendering's emphasis on artistic representation might introduce inaccuracies in anatomical details. The artistic enhancements applied during rendering might introduce an unobjective element, potentially influencing interpretations. Addressing these limitations will be crucial to unlocking cinematic rendering's full potential in clinical, educational, and research contexts as technology advances.

Another aspect concerns the study of internal structure. Many medical image viewers enable the visualization of section images, allowing the simultaneous study of volume rendering results and sections in various planes, such as orthogonal or curved MPR. These multiplanar reformations enable the display of the appearance of internal structures on different cutting planes and easy navigation. While achievable, such studies are more complex to be performed with anatomical specimens as they require serial physical sectioning or partial destruction.

A third aspect pertains to technical feasibility factors. Acquiring and processing CT and MRI data demands advanced technical expertise. Volume rendering of internal anatomical structures from radiological images necessitates prior segmentation. Automatic routines or segmentation assistance can achieve segmentation when the structure stands out from its surroundings, for instance, the vascular tree highlighted by iodinated contrast product in CT scans or by paramagnetic contrast or time-of-flight effects in MRI. However, manual segmentation is still mandatory for correctly reconstructing many structures, which can be labor-intensive and time-consuming. This step is circumvented in post-mortem imaging of extracted anatomical specimens and in photogrammetry.

Both volumetric imaging and 3D photogrammetry have distinct advantages and disadvantages in teaching anatomy. In many health

science curricula, progressive exposure to different methods of illustrating anatomy is necessary: simplified schemes, drawings, cadaveric dissections, and medical images. These different modalities have different objectives and are not self-excluding. While 3D techniques using CT or MRI datasets provide a view of internal structures, smartphone-based 3D photogrammetry offers realism and accessibility. The choice between these techniques will depend on educational objectives, available resources, and specific curriculum needs. Combining these approaches can enrich students' learning experience by providing a more comprehensive and realistic view of the human body.

As with any imaging technique, smartphone-based photogrammetry presents limitations. All aspects of the specimens can be obtained by multiple fused acquisitions, but the reconstruction of fused areas may not be perfect in areas of shadows. Consequently, the use of a relatively homogeneous light in the room where the procedure is performed is important. A strength of this technique is that it represents a major advance in the accessibility of creating and sharing realistic 3D anatomical models. Given its simplicity and affordability, it is likely to be easily popularized and developed further.

## CONCLUSION

In the present study, we assessed an innovative approach to anatomical education by synthesizing smartphone-based 360° photogrammetry, virtual camera recording, and stereoscopic display to craft lifelike 3D anatomical models. The results unequivocally demonstrate the viability and effectiveness of this methodology across different types of anatomical specimens, encompassing osteological, soft organ, neuroanatomical, regional dissection, and a dedicated 3D-printed phantom test. Among the key findings, the resulting 3D models exhibited photorealistic textures closely resembling the actual structures. However, occasional imperfections were discerned due to variations in lighting conditions during image acquisition. The photogrammetry technique adeptly fused images, eliminating extraneous backgrounds and facilitating comprehensive specimen capture. It effectively replicated the morphological complexity of the studied specimens and rendered all 3D anatomical models in both red-cyan anaglyph and side-by-side stereoscopic modes, enhancing depth perception, which has the potential to improve the educational experience.

The entire process, from image capture to stereoscopic file export, proved to be straightforward and cost-effective, eliminating the need for expensive equipment and ensuring applicability across diverse educational environments. This approach holds significant promise for advancing anatomical education by simultaneously providing accessibility, realism, and versatility. Smartphone-based 360° photogrammetry represents a groundbreaking avenue for anatomical education as it democratizes access to the production of high-fidelity, shareable 3D anatomical models.

## ACKNOWLEDGMENTS

The authors sincerely thank those who donated their bodies to science so that anatomical research could be performed. Research plays a central role in advancing patient care by enriching our knowledge base. Therefore, the donors and their families deserve our highest gratitude. The authors also thank Carine Beausse, Jérôme Machut, and Gérald Deluermoz, members of the anatomy laboratory staff, for their assistance, and Daniel Bourry, Director of Digital and Multimedia Production of the University of Tours School of Medicine, for his invaluable advices in the field of photography.

## CONFLICT OF INTEREST STATEMENT

The authors declare that they have no conflict of interest.

## ETHICS STATEMENT

The authors state that every effort was made to follow all local and international ethical guidelines and laws pertaining to using human cadaveric donors in anatomical research.

## ORCID

Alex Morichon  <https://orcid.org/0009-0001-5562-0149>

Guillaume Dannhoff  <https://orcid.org/0000-0002-2822-0035>

Laurent Barantin  <https://orcid.org/0000-0002-5119-658X>

Christophe Destrieux  <https://orcid.org/0000-0001-5348-8052>

Igor Lima Maldonado  <https://orcid.org/0000-0001-6037-0407>

## REFERENCES

1. Triepels CPR, Smeets CFA, Notten KJB, Kruitwagen RFP, Futterer JJ, Vergeldt TFM, et al. Does three-dimensional anatomy improve student understanding? *Clin Anat*. 2020;33:25–33.
2. Asad MR, Asghar A, Tadvi N, Ahmed MM, Nazeer M, Amir KM, et al. Medical faculty perspectives toward cadaveric dissection as a learning tool for anatomy education: a survey study in India. *Cureus*. 2023. in press. <https://doi.org/10.7759/cureus.37713>
3. Asante EA, Maalman RS, Ali MA, Donkor YO, Korpisah JK. Perception and attitude of medical students towards cadaveric dissection in anatomical science education. *Ethiop J Health Sci*. 2021;31:867–74.
4. Kochhar S, Tasnim T, Gupta A. Is cadaveric dissection essential in medical education? A qualitative survey comparing pre-and post-COVID-19 anatomy courses. *J Osteopath Med*. 2022;123:19–26.
5. Ghosh SK. Lacunae regarding dearth of dissection-based teaching during COVID-19 pandemic: how to cope with it? *Surg Radiol Anat*. 2022;44:75–9.
6. Rockarts J, Brewer-Deluce D, Shali A, Mohialdin V, Wainman B. National survey on Canadian undergraduate medical programs: the decline of the anatomical sciences in Canadian medical education. *Anat Sci Educ*. 2020;13:381–9.
7. Shichinohe T, Kondo T, Date H, Hiramatsu M, Hirano S, Ide C, et al. Guidelines for cadaver dissection in education and research of clinical medicine (the Japan surgical society and the Japanese Association of Anatomists). *Anat Sci Int*. 2022;97:235–40.
8. Erolin C. Interactive 3D digital models for anatomy and medical education. In: Rea PM, editor. *Biomedical visualisation*. Cham: Springer International Publishing; 2019a. p. 1–16.
9. Rubio RR, Shehata J, Kournoutas I, Chae R, Vigo V, Wang M, et al. Construction of neuroanatomical volumetric models using 3-dimensional scanning techniques: technical note and applications. *World Neurosurg*. 2019;126:359–68.

10. Testut L, Jacob O. *Traité d'anatomie topographique, avec applications médico-chirurgicales. Abdomen. Bassin. Membres.* 4th ed. Paris: Librairie Octave Doin; 1921.
11. Gurses ME, Gungor A, Rahmanov S, Gökalp E, Hanalioglu S, Berker M, et al. Three-dimensional modeling and augmented reality and virtual reality simulation of fiber dissection of the cerebellum and brainstem. *Oper Neurosurg.* 2022;23:345–54.
12. Spiriev T, Mitev A, Stoykov V, Dimitrov N, Maslarski I, Nakov V. Three-dimensional immersive photorealistic layered dissection of superficial and deep back muscles: anatomical study. *Cureus.* 2022. in press. <https://doi.org/10.7759/cureus.26727>
13. Raja B, Chandra A, Azam M, Das S, Agarwal A. Anatomage—the virtual dissection tool and its uses: a narrative review. *J Postgrad Med.* 2022;68:156–61.
14. Tomlinson SB, Hendricks BK, Cohen-Gadol A. Immersive three-dimensional modeling and virtual reality for enhanced visualization of operative neurosurgical anatomy. *World Neurosurg.* 2019a;131:313–20.
15. Pereira N, Kufeke M, Parada L, Troncoso E, Bahamondes J, Sanchez L, et al. Augmented reality microsurgical planning with a smartphone (ARM-PS): a dissection route map in your pocket. *J Plast Reconstr Aesthetic Surg.* 2019;72:759–62.
16. Silén C, Wirell S, Kvist J, Nylander E, Smedby O. Advanced 3D visualization in student-centred medical education. *Med Teach.* 2008;30:e115–e124.
17. Falkingham P. Acquisition of high resolution three-dimensional models using free, open-source, photogrammetric software. *Palaeontol Electron.* 2012. in press. <https://doi.org/10.26879/264>
18. Mallison H, Wings O. Photogrammetry in paleontology—a practical guide. *J Paleontol Tech.* 2014;12:1–31.
19. Morgan B, Ford ALJ, Smith MJ. Standard methods for creating digital skeletal models using structure-from-motion photogrammetry. *Am J Phys Anthropol.* 2019;169:152–60.
20. Łabędź P, Skabek K, Ozimek P, Rola D, Ozimek A, Ostrowska K. Accuracy verification of surface models of architectural objects from the iPad LiDAR in the context of photogrammetry methods. *Sensors.* 2022;22:8504.
21. Aydin SO, Barut O, Yilmaz MO, Sahin B, Akyoldas G, Akgun MY, et al. Use of 3-dimensional modeling and augmented/virtual reality applications in microsurgical neuroanatomy training. *Oper Neurosurg.* 2023;24:318–23.
22. Gianotto I, Coutts A, Pérez-Pachón L, Gröning F. Evaluating a photogrammetry-based video for undergraduate anatomy education. In: Border S, Rea PM, Keenan ID, editors. *Biomedical visualisation.* Cham: Springer International Publishing; 2023. p. 63–78.
23. de Oliveira ASB, Leonel LCPC, LaHood ER, Hallak H, Link MJ, Maleszewski JJ, et al. Foundations and guidelines for high-quality three-dimensional models using photogrammetry: a technical note on the future of neuroanatomy education. *Anat Sci Educ.* 2023. in press. <https://doi.org/10.1002/ase.2274>
24. To JK, Wang JN, Vu AN, Ediriwickrema LS, Browne AW. Optimization of a novel automated, low cost, three-dimensional photogrammetry system (PHACE). *medRxiv [Preprint].* 2023;2023.04.21.23288659. <https://doi.org/10.1101/2023.04.21.23288659>
25. Iwanaga J, Terada S, Kim H, Tabira Y, Arakawa T, Watanabe K, et al. Easy three-dimensional scanning technology for anatomy education using a free cellphone app. *Clin Anat.* 2021;34:910–8.
26. Ille S, Ohlerth A-K, Colle D, Colle H, Dragoy O, Goodden J, et al. Augmented reality for the virtual dissection of white matter pathways. *Acta Neurochir.* 2021;163:895–903.
27. Palmer EG, Reddy RK, Laughy W. Teaching professionalism to medical students using dissection-based anatomy education: a practical guide. *Med Sci Educ.* 2021;31:203–13.
28. Roh TH, Oh JW, Jang CK, Choi S, Kim EH, Hong C-K, et al. Virtual dissection of the real brain: integration of photographic 3D models into virtual reality and its effect on neurosurgical resident education. *Neurosurg Focus.* 2021;51:E16.
29. Jędrzejewski Z, Loranger B, Clancy JA. Virtual anatomy museum: facilitating public engagement through an interactive application. In: Rea PM, editor. *Biomedical visualisation.* Cham: Springer International Publishing; 2020. p. 1–18.
30. Wesencraft KM, Clancy JA. Using photogrammetry to create a realistic 3D anatomy learning aid with unity game engine. In: Rea PM, editor. *Biomedical visualisation.* Cham: Springer International Publishing; 2019. p. 93–104.
31. Frithioff A, Freund M, Weiss K, Foghsgaard S, Pedersen DB, Sørensen MS, et al. Effect of 3D-printed models on cadaveric dissection in temporal bone training. *OTO Open.* 2021;5:2473974X211065102.
32. Lim KHA, Loo ZY, Goldie SJ, Adams JW, McMenamin PG. Use of 3D printed models in medical education: a randomized control trial comparing 3D prints versus cadaveric materials for learning external cardiac anatomy. *Anat Sci Educ.* 2016;9:213–21.
33. McMenamin PG, Quayle MR, McHenry CR, Adams JW. The production of anatomical teaching resources using three-dimensional (3D) printing technology. *Anat Sci Educ.* 2014;7:479–86.
34. Hojo D, Muroto K, Nozawa H, Kawai K, Hata K, Tanaka T, et al. Utility of a three-dimensional printed pelvic model for lateral pelvic lymph node dissection education: a randomized controlled trial. *J Am Coll Surg.* 2019;229:552–9. e3.
35. Salazar DA, Cramer J, Markin NW, Hunt NH, Linke G, Siebler J, et al. Comparison of 3D printed anatomical model qualities in acetabular fracture representation. *Ann Transl Med.* 2022;10:391.
36. Davidson JM. Remarks on the value of stereoscopic photography and skiagraphy: records of clinical and pathological appearances. *Br Med J.* 1898;2(1979):1669.
37. Basset DL, Gruber WB. *A stereoscopic atlas of human anatomy.* Portland: Sawyer's Inc; 1962.
38. Lechanoine F, Smirnov M, Armani-Franceschi G, Carneiro P, Cottier P, Destrieux C, et al. Stereoscopic images from computed tomography angiograms. *World Neurosurg.* 2019;128:259–67.
39. Prentice ED, Metcalf WK, Quinn TH, Sharp JG, Jensen RH, Holyoke EA. Stereoscopic anatomy: evaluation of a new teaching system in human gross anatomy. *J Med Educ.* 1977;52:758–63.
40. Getty DJ, Green PJ. Clinical applications for stereoscopic 3-D displays. *J Soc Inf Disp.* 2007;15:377–84.
41. Nam KW, Park J, Kim IY, Kim KG. Application of stereo-imaging technology to medical field. *Healthc Inform Res.* 2012;18:158.
42. Ammanuel S, Brown I, Uribe J, Rehani B. Creating 3D models from radiologic images for virtual reality medical education modules. *J Med Syst.* 2019;43:166.
43. Anastasi G, Bramanti P, Di Bella P, Favalaro A, Trimarchi F, Magaudo L, et al. Volume rendering based on magnetic resonance imaging: advances in understanding the three-dimensional anatomy of the human knee. *J Anat.* 2007;211:399–406.
44. Chang C-W, Atkinson G, Gandhi N, Farrell ML, Labrash S, Smith AB, et al. Cone beam computed tomography of plastinated hearts for instruction of radiological anatomy. *Surg Radiol Anat.* 2016;38:843–53.
45. Fan KS, Durnea C, Nygaard CC, Khalil M, Doumouchsis SK. Three-dimensional volume rendering of pelvic floor anatomy with focus on fibroids in relation to the lower urogenital tract based on cross-sectional MRI images. *J Med Syst.* 2023;47:62.
46. Fasel JHD, Aguiar D, Kiss-Bodolay D, Montet X, Kalangos A, Stimec BV, et al. Adapting anatomy teaching to surgical trends: a combination of classical dissection, medical imaging, and 3D-printing technologies. *Surg Radiol Anat.* 2016;38:361–7.
47. Keenan ID, Ben AA. Integrating 3D visualisation technologies in undergraduate anatomy education. In: Rea PM, editor. *Biomedical visualisation.* Cham: Springer International Publishing; 2019. p. 39–53.
48. Lee H, Kim J, Cho Y, Kim M, Kim N, Lee K. Three-dimensional computed tomographic volume rendering imaging as a teaching tool in veterinary radiology instruction. *Vet Med.* 2010;55:603–9.

49. Mei X, Atturo F, Wadin K, Larsson S, Agrawal S, Ladak HM, et al. Human inner ear blood supply revisited: the Uppsala collection of temporal bone—an international resource of education and collaboration. *Ups J Med Sci*. 2018;123:131–42.
50. Murakami T, Tajika Y, Ueno H, Awata S, Hirasawa S, Sugimoto M, et al. An integrated teaching method of gross anatomy and computed tomography radiology: anatomy-CT integrated education. *Anat Sci Educ*. 2014;7:438–49.
51. Venail F, Deveze A, Lallemand B, Guevara N, Mondain M. Enhancement of temporal bone anatomy learning with computer 3D rendered imaging softwares. *Med Teach*. 2010;32:e282–e288.
52. Binder J, Krautz C, Engel K, Grützmann R, Fellner FA, Burger PHM, et al. Leveraging medical imaging for medical education—a cinematic rendering-featured lecture. *Ann Anat*. 2019;222:159–65.
53. Eid M, De Cecco CN, Nance JW, Caruso D, Albrecht MH, Spandorfer AJ, et al. Cinematic rendering in CT: a novel, lifelike 3D visualization technique. *Am J Roentgenol*. 2017;209:370–9.
54. Niedermair JF, Antipova V, Manhal S, Siwetz M, Wimmer-Röll M, Hammer N, et al. On the added benefit of virtual anatomy for dissection-based skills. *Anat Sci Educ*. 2023;16:439–51.

## AUTHOR BIOGRAPHIES

**Alex Morichon** holds a Master of Science in Anatomy and Biomedical Research in Body Donors and is a medical student at the University of Tours, France. He conducts research at the iBrain Laboratory (U1253) of the French National Institute of Health and Medical Research, focusing on anatomy education and intrinsic cerebral anatomy. He has been serving as a monitor for the human anatomy course, mentoring younger students, for over 2 years.

**Guillaume Dannhoff** holds a Master of Science in Surgical Sciences/Neurosciences and is a medical resident in Neurological Surgery at the University of Strasbourg, France. He conducts research at the iBrain Laboratory (U1253) of French National Institute of Health and Medical Research in Tours, France, focusing on neuroanatomy, anatomy teaching, and oncological neurosurgery. He has been mentoring younger students as an anatomy tutor and dissection monitor for over 8 years.

**Laurent Barantin** holds a Ph.D. in Life and Health Sciences/Medical Imaging and is a Research Engineer at the University of Tours, France, in charge of magnetic resonance methodological developments. He conducts research at the iBrain Laboratory (U1253) of the French Institute of Medical and Scientific Research, focusing on *in vivo* and *ex vivo* imaging and the development of innovative methods to test the accuracy and precision of neuroimaging and stereotactic techniques. He has been instructing students in the master's degree program for medical imaging at the University of Tours for over 20 years.

**Christophe Destrieux** holds a Ph.D. in Health, Science, and Technologies. He is a neurosurgeon and professor of anatomy at the University of Tours, France. He is the head of the body donation program at the University of Tours Medical School and conducts research at the iBrain Laboratory (U1253) of the French Institute of Medical and Scientific Research, focusing on neuroanatomy, *in vivo* and *ex vivo* imaging, as well as atlases building. In addition to his regular teaching duties, he has been instructing neuroanatomy in the European Association of Neurosurgical Societies training courses for over 20 years.

**Igor Lima Maldonado** holds a Ph.D. in Life and Health Sciences/Neurosciences. He is a neurosurgeon and professor of anatomy at the Federal University of Bahia, Salvador, Brazil, in mobility at the University of Tours and the iBrain Laboratory (U1253) of the French Institute of Medical and Scientific Research, Tours, France. His works focus on neuroanatomy, cerebral white matter and vascularization, and the development of innovative methods for acquiring surface data for research and educational purposes. In addition to his regular teaching duties, he has been instructing neuroanatomy in the World Federation of Neurosurgical Societies and the International Academy of Neurosurgical Anatomy courses for over 10 years.

## SUPPORTING INFORMATION

Additional supporting information can be found online in the Supporting Information section at the end of this article.

**How to cite this article:** Morichon A, Dannhoff G, Barantin L, Destrieux C, Maldonado IL. Doing more with less: Realistic stereoscopic three-dimensional anatomical modeling from smartphone photogrammetry. *Anat Sci Educ*. 2024;00:1–14. <https://doi.org/10.1002/ase.2402>